Available online at www.sciencedirect.com
ScienceDirect
Solar Energy Materials & Solar Cells 91 (2007) 924–930
Solar Energy Materials and Solar Cells
www.elsevier.com/locate/solmat

Plasma-enhanced chemical vapor deposition of zinc oxide at atmospheric pressure and low temperature

M.D. Barankin, E. Gonzalez II, A.M. Ladwig, R.F. Hicks*

Department of Chemical and Biomolecular Engineering, University of California, Los Angeles, Box 951592, Los Angeles, CA 90095-1592, USA

Received 15 September 2006; received in revised form 23 January 2007; accepted 14 February 2007
Available online 6 April 2007

Abstract

The plasma-enhanced chemical vapor deposition of aluminum-doped zinc oxide has been demonstrated for the first time at 800 Torr and under 250 °C. A film resistivity of $3\times10^{-2}\,\Omega$cm and a transparency of 95% from 375 to 2500 nm was obtained for deposition at 20-mTorr diethylzinc, 1.0 Torr CO_2, 799 Torr He, a TMAl/DEZn ratio of 1:100, 41 W/cm^3 RF power, and 225 °C. The average aluminum concentration in the ZnO film was 5.4×10^{20} cm^{-3}. It was found that, while the growth rate did not change with substrate temperature, both the resistivity and optical absorption coefficient declined with increasing temperature.
© 2007 Elsevier B.V. All rights reserved.

Keywords: Transparent-conducting oxide (TCO); Al/ZnO; PECVD

1. Introduction

Aluminum-doped zinc oxide is a promising material for the transparent-conducting layer in photovoltaic devices. Zinc oxide has been grown by vacuum sputtering [1,2], thermal chemical vapor deposition (CVD) [3], plasma-enhanced chemical vapor deposition (PECVD) [4], expanding thermal plasma [5], and vacuum arc deposition [6]. Most of these processes are performed under vacuum in batch process chambers. In order to reduce the cost of producing thin-film photovoltaics, it is desirable to develop alternative processes that operate at atmospheric pressure and can be applied to continuous, in-line manufacturing.

Atmospheric pressure CVD has been used to produce textured Al/ZnO to serve as a back reflector for photovoltaic devices. It has been reported that this process yields material with a resistivity of $1\times10^{-3}\,\Omega$cm and transparency of 80%–90%. The substrate temperature needed to achieve these results was 400 °C [7]. Although these material properties are acceptable, there is a need to further reduce the temperature to allow for the deposition on thermally sensitive materials, such as copper indium gallium diselenide (CIGS) or plastic substrates [1,2,8].

In this paper, we report on the deposition of aluminum-doped zinc oxide films utilizing atmospheric pressure plasma. The plasma was generated by flowing helium and carbon dioxide, or oxygen, through two closely spaced electrodes that were connected to a radio-frequency (RF) power supply. The chemical precursors, diethylzinc and trimethylaluminum, were mixed with the plasma just downstream of the electrodes, and then directed onto glass or silicon substrates heated to between 200 and 235 °C. The precursors decomposed in the presence of the reactive gas and formed the ZnO films. In earlier studies, this novel plasma source has been used to grow amorphous hydrogenated silicon [9], silicon dioxide [10], and silicon nitride [11]. Herein, we examine the potential of atmospheric pressure PECVD for the deposition of aluminum-doped zinc oxide at low temperature.

2. Experimental methods

A schematic of the plasma source is shown in Fig. 1. It consisted of two perforated aluminum electrodes, 33 mm in diameter, separated by a gap 1.6 mm wide (Atomflo™-250D from Surfx Technologies). The electrodes were perforated to allow helium and either carbon dioxide or oxygen to flow through them. The upper electrode was

*Corresponding author. Tel.: +1 310 206 6865; fax: +1 310 206 4107.
E-mail address: rhicks@ucla.edu (R.F. Hicks).

0927-0248/$ - see front matter © 2007 Elsevier B.V. All rights reserved.
doi:10.1016/j.solmat.2007.02.009

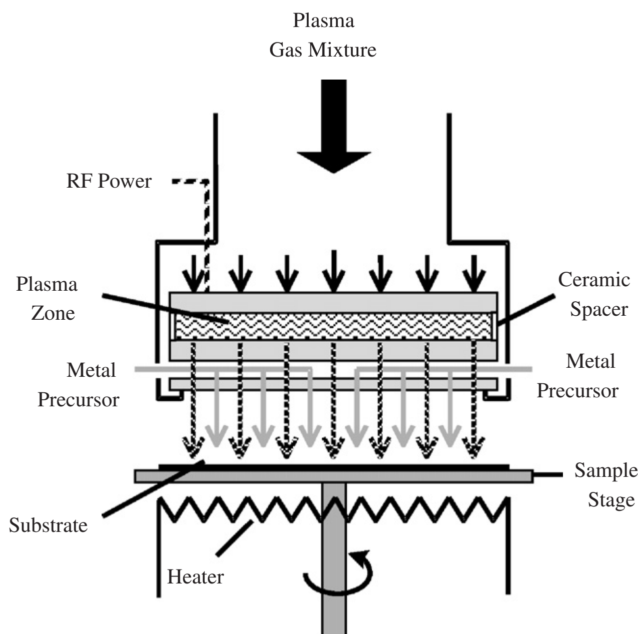

Fig. 1. Schematic of the atmospheric plasma source and substrate holder.

connected to an RF power supply at 13.56 MHz, while the lower electrode was grounded. A third aluminum plate was installed beneath the lower electrode. It contained a network of channels and holes that mixed the metalorganic precursors with the plasma afterglow. Located 4 mm further downstream was a rotating sample stage with integrated heating system.

The plasma was fed with 30 L/min of ultrahigh purity helium (99.999%), and 44 cm^3/ min of either medical grade carbon dioxide (99.8%) or ultrahigh purity oxygen (99.999%). Diethylzinc (DEZn) and trimethylaluminum (TMAl) were stored in stainless steel bubblers that were placed in baths maintained at 26.0 and 16.7 °C, respectively. The bubbler pressures were fixed at 1160 and 1100 Torr, respectively, using MKS pressure controllers with Baratron sensors. The helium was further purified by an SAES pure-gas monotorr purifier to reduce the oxygen concentration below 1 ppb before entering the flow system. A dilution flow rate of 5.5 L/min was added to the precursor delivery lines downstream of the bubblers to improve the mixing in the showerhead. The substrates used were Corning 1737 glass coupons, $3.8 \times 3.8\,cm^2$, or silicon (1 0 0) wafers, 10 cm in diameter. Since the diethylzinc reacts rapidly with oxygen, films grown by thermal CVD with O_2 were compared to those grown by PECVD with CO_2.

The films were deposited by PECVD or thermal CVD using the procedure given below. Thermal CVD differed from PECVD only in that the plasma was extinguished prior to the introduction of the precursors. The substrate was washed in de-ionized water and acetone, dried with compressed air, and baked in a fume hood at 300 °C for 5 min before being placed on the sample holder. The chamber was evacuated to a pressure of 30 mTorr, and then pressurized with helium to 800 Torr. After heating the substrate to the growth temperature while spinning at 150 rpm, a glow discharge was struck with 75 W of RF power. After 4 min of operation, the carbon dioxide or oxygen flow was introduced. Then deposition was initiated by feeding 47 to 165 cm^3/ min of helium to the diethylzinc bubbler, and 1.3 cm^3/ min of helium to the trimethylaluminum bubbler. The corresponding partial pressures were 20–70 mTorr of diethylzinc and 0.2 mTorr of trimethylaluminum. At the end of the deposition time, the precursor flow was switched to a vent line, and after one additional minute, the dilution flow was switched off and the plasma extinguished.

Film thickness measurements were performed using a Veeco Dektak 8 profilometer. A step was created in the film by masking a radial sector of the substrate, and then etching with 0.1 M nitric acid. To calculate the average growth rate an integrated average was calculated from 69 thickness measurements, made with a spacing of 0.72 mm along the radius. This thickness value was divided by the total deposition time. In addition, maximum growth rates were calculated by dividing the thickest region on a sample by the deposition time. In separate experiments, it was confirmed that the rate remained constant over growth periods from 0 to 45 min.

Sheet resistance measurements were taken on 4 in silicon substrates using a Prometrix 4-point probe. These values were multiplied by the film thickness to obtain the resistivity. The optical absorbance of films grown on glass coupons was measured using a Hitachi U-3410 spectrophotometer with tungsten halogen and deuterium lamps. Average absorbances were calculated by averaging the measured absorbance from 375 to 2500 nm. Absorption coefficients were obtained by dividing the average absorbance by the average film thickness. The bulk composition of an aluminum-doped zinc oxide film was examined by secondary ion mass spectroscopy with depth profiling at the Charles Evans Analytical Group. Only one location was measured by SIMS, on the lowest resistivity film, with a spot size of 50 μm. Film morphology was examined using a Hitachi S4700 field-emission scanning electron microscope (SEM). Cross-sectional electron micrographs were taken at an incidence angle of $\leqslant 1°$.

3. Results

3.1. Plasma-enhanced and thermal CVD using O_2 and CO_2

A comparison of the radial thickness profiles of zinc oxide films grown by four different methods is depicted in Fig. 2. The process conditions for thermal CVD were 40-mTorr diethylzinc, 0.5 Torr O_2, or 1.0 Torr CO_2, 800 Torr total pressure, and 181 °C. For PECVD, the same conditions were used, except with 50 W of RF power applied to the plasma source. It is found that the film thickness profiles exhibit maxima at a radial position near the outer edge of the plasma source, suggesting that the

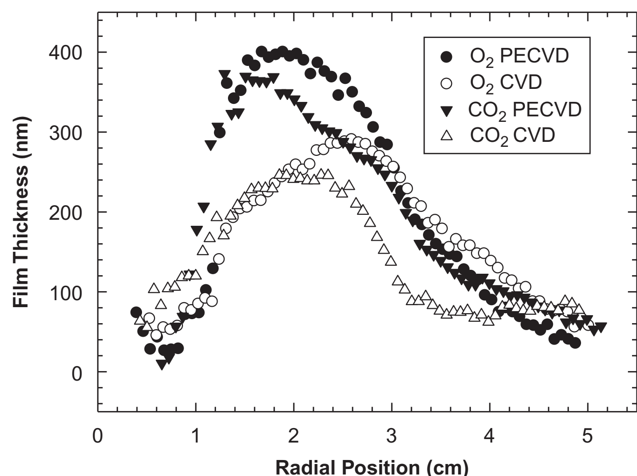

Fig. 2. Radial thickness profiles for films grown by PECVD and CVD with O_2 and CO_2.

diethylzinc is not transported efficiently to the center of the showerhead prior to exiting the source, i.e., to radii below 1.0 cm. One can see that the amount of material deposited by PECVD is higher than that observed by CVD. This difference amounts to the contribution that the plasma-initiated reaction contributes to the overall deposition process. The ratio of the area under the profiles for PECVD versus CVD equals 1.5 when carbon dioxide is the reactive gas and 1.1 when oxygen is the reactive gas. The ratio of the maximum film thickness to the average film thickness is 2.2 for ZnO deposited by PECVD with CO_2. Previous research on the atmospheric pressure plasma source has shown that the plasma is homogeneous within the gas volume between the electrodes [12], so it is likely that the non-uniform mixing of the precursor in the showerhead is responsible for the wide variation in film thickness across the wafer.

Listed in Table 1, are the results of a mass balance analysis for the PECVD and CVD reactions, using the same process conditions as given in the preceding paragraph. The zinc in the film is calculated from the volume of the deposit times an assumed density of 5.6 g/cm^3 [13]. The deposition efficiency is obtained by dividing the Zn in the film by the amount of Zn fed to the reactor. The film deposited by PECVD with O_2 exhibited an average growth rate of 37 nm/min, and a deposition efficiency of 17%. Films grown by PECVD with carbon dioxide or CVD with oxygen yielded slightly lower growth rates of 33 nm/min, and the same deposition efficiency. On the other hand, thermal CVD with CO_2 exhibited the lowest growth rate and efficiency, most likely due to the lower reactivity of carbon dioxide with diethylzinc.

3.2. Average growth rate

The dependence of the average growth rate of ZnO on diethylzinc partial pressure during the PECVD process is depicted in Fig. 3. The conditions were 5.0 Torr CO_2, 800 Torr total pressure, 40 W RF power, and 100 °C substrate temperature. The growth rate increases rapidly as the diethylzinc partial pressure is raised from 20 to 60 Torr. Thereafter it levels off to 120 nm/min at the higher partial pressures. The maximum deposition rate recorded on the wafer at 70 mTorr of diethylzinc was ~200 nm/ min at a radial position of 2 cm on the wafer. The two data sets shown in the figure correspond to separate runs before and after introduction of a zero-dead-volume flow manifold for switching the precursor feed between the reactor and the bypass lines.

Table 1
Mass balance for ZnO grown by PECVD and CVD with O_2 and CO_2

	PECVD		CVD	
	O_2	CO_2	O_2	CO_2
G_R (±0.2 nm/ min)	37.1	33.2	33.3	24.8
Zn in film (±0.03 mg)	6.22	6.18	5.89	4.23
Dep. efficiency (±0.1%) (%)	16.9	16.8	16.1	11.5

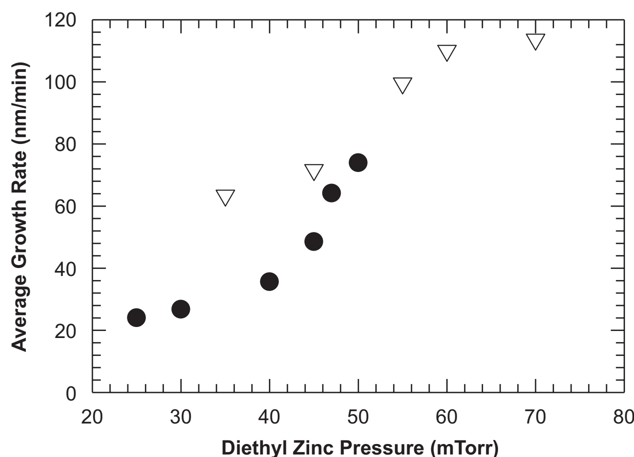

Fig. 3. Dependence of the average growth rate on the DEZn partial pressure for two separate runs, before (●) and after (▽) installation of a new flow manifold.

3.3. Properties of Al-doped ZnO films

In Fig. 4, the dependence of the average film resistivity on substrate temperature is shown for PECVD with 1.0 Torr of CO_2 and CVD with 1.0 Torr of O_2. For the PECVD process, two different diethylzinc partial pressures were examined, 20 and 60 mTorr, while only 20 mTorr of DEZn was used in the CVD experiments. In all the 60-mTorr runs, TMAl was fed to the reactor at a ratio of Al to Zn of 1–300, whereas a ratio of 1 to 100 was used for the 20-mTorr runs. These films exhibited a non-uniform radial distribution of film thickness analogous to that seen in Fig. 2. All films grown by CVD with O_2, except the film grown at the highest substrate temperature, have a resistivity that is outside the range of the 4-point probe. By contrast, ZnO films grown by PECVD with CO_2 exhibit

much lower resistivities at the same temperature. For these samples, the resistivity decreases with decreasing DEZn partial pressure and increasing substrate temperature, with the latter variable dominating the trend. For PECVD at the highest substrate temperature examined, i.e., 224 °C, the average film resistivity is $2.9 \times 10^{-2}\,\Omega\,cm$. Note that for these samples the average growth rate is near 20 nm/min. We expect that if the substrate temperature were to be raised above 225 °C, the film resistivity would continue to fall. This trend is in agreement with results reported in literature for vacuum deposition processes [4,5,8].

Shown in Fig. 5 is an SIMS profile of Al and Zn for a film deposited by PECVD with CO_2 using 20 mTorr of diethylzinc and 224 °C. This film has an average resistivity of $3.3 \times 10^{-2}\,\Omega\,cm$. The resistivity in the sputtered region is $1.2 \times 10^{-2}\,\Omega\,cm$. This figure shows that the Al concentration peaks near the surface of the film at $1.7 \times 10^{21}\,cm^{-3}$. This value exceeds the theoretical maximum in carrier concentration of$1.5 \times 10^{21}\,cm^{-3}$ [14]. The average concentration throughout the 1350-nm-thick film is approximately $5.4 \times 10^{20}\,cm^{-3}$. Based on the resistivity measured for the Al-doped ZnO film, it is estimated that less than 10% of the aluminum atoms are electrically active. Since the SIMS measurement was made at only one position on the sample, no conclusion can be drawn about the distribution of aluminum across the wafer.

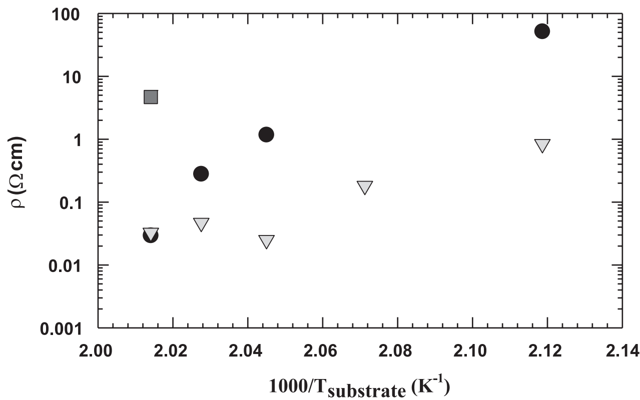

Fig. 4. Dependence of the film resistivity on temperature for PECVD with CO_2 at 20 (▼) and 60 (●) mTorr of DEZn and CVD with O_2 at 20 mTorr of DEZn (■).

Presented in Fig. 6 is the dependence of the average absorption coefficient of the Al-doped ZnO films grown by PECVD and CVD as a function of substrate temperature. The films were deposited on glass coupons to an average thickness of 500 nm under the following conditions: 1.0 Torr CO_2 or O_2, 800 Torr total pressure, a TMAl/DEZn feed ratio of 1:100, and 50 W RF power for the PECVD experiments. The data in Fig. 6 reveal that the absorbance decreases with increasing substrate temperature and decreasing diethylzinc partial pressure. The lowest average absorption coefficient (highest relative transparency) is achieved by PECVD with CO_2 at 20-mTorr diethylzinc and 224 °C, $a = 0.04\,\mu m^{-1}$. For the same process conditions, the absorption coefficient values for ZnO grown by CVD are roughly double that of the ZnO film grown by PECVD. These results, together with the resistivity data presented above, demonstrate that the atmospheric pressure plasma process provides improved material properties at low deposition temperatures.

3.4. Film morphology

The Al-doped ZnO film that exhibits a resistivity of $3.3 \times 10^{-2}\,\Omega\,cm$ was analyzed by SEM. An image of this sample is shown in Fig. 7. The surface of the film is smooth and continuous. The cleaved edge of the film shows that it contains vertical columnar grains that extend from the substrate up to the surface. The average grain size is estimated to be 150 nm. Further note that the surface of the cleaved edge of the film is relatively rough, and suggests that there could be some voids interspersed between the large grains.

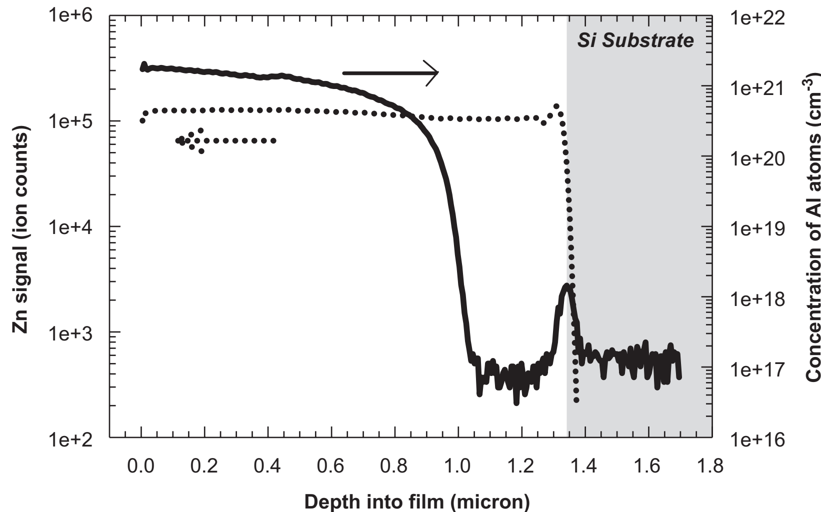

Fig. 5. SIMS depth profile of Al and Zn in a doped ZnO film grown by PECVD with CO_2 at 224 °C.

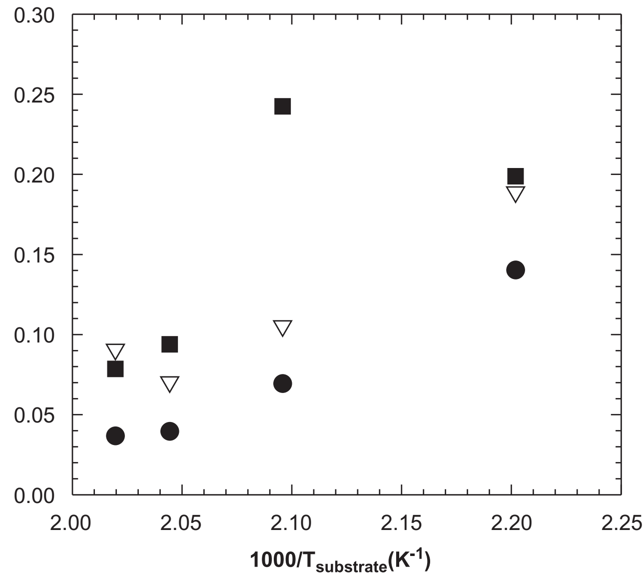

Fig. 6. Absorption coefficients for films grown by CVD with O_2 at 20 mTorr of DEZn (■) and PECVD with CO_2 at 20 (●) and 60 (▽) mTorr of DEZn.

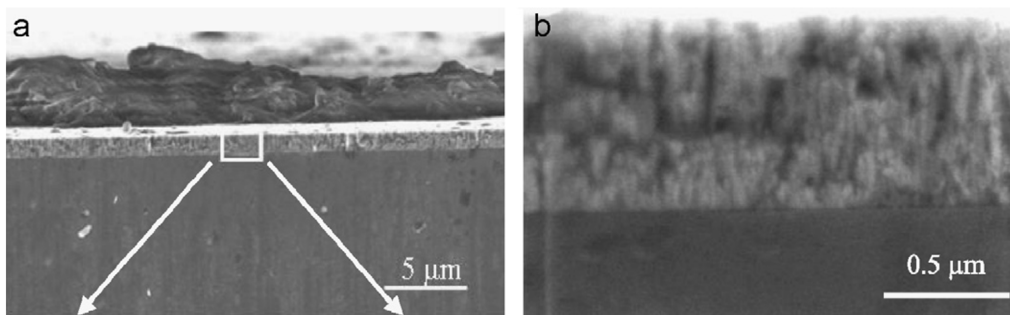

Fig. 7. Scanning electron micrograph of an Al-doped ZnO film grown by PECVD with CO_2 at 224 °C: (a) 5.0 µm and (b) 0.5 µm resolution.

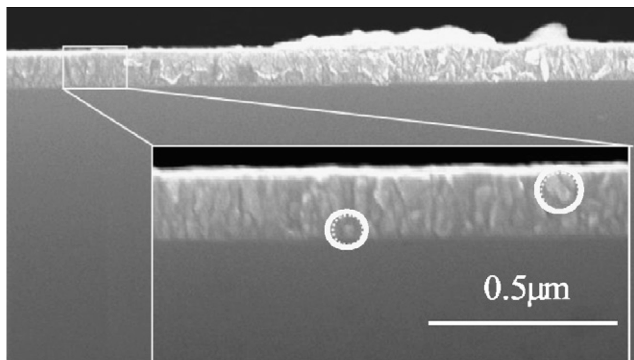

Fig. 8. Scanning electron micrograph of an Al-doped ZnO film grown by CVD with O_2 at 224 °C.

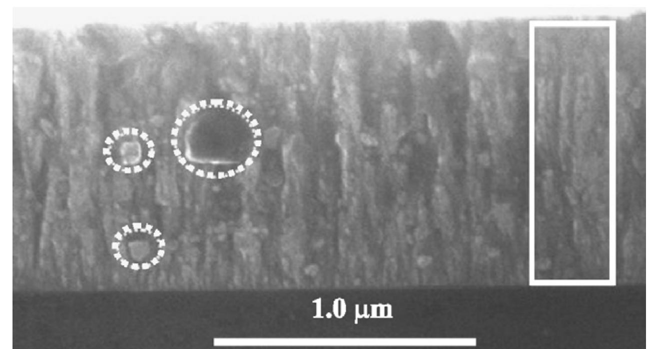

Fig. 9. Scanning electron micrograph of an Al-doped ZnO film grown by PECVD with CO_2 at 199 °C.

Presented in Fig. 8 is an SEM image of an Al-doped zinc oxide film grown by CVD at 1.0 Torr O_2, 20-mTorr diethylzinc, and 224 °C. This material exhibits a high resistivity of 4.7 Ω cm, but the Al concentration is unknown as SIMS analysis was not performed on this sample. The principal difference that can be discerned between this ZnO film and the film of much lower resistivity (cf. Fig. 7) is the presence of small circular grains that disrupt the vertical columnar growth morphology. Two of these circular grains are highlighted with dashed white circles in the image.

An electron micrograph of an Al-doped zinc oxide film grown by PECVD at 1.0 Torr CO_2, 60-mTorr diethylzinc, and 199 °C is shown in Fig. 9. This material exhibits an average resistivity of 52 Ω cm. The image shows some regions of vertical columnar structure, as indicated by the white rectangle on the right side. However, there are many small circular grains ranging in size from 10 to 300 nm in

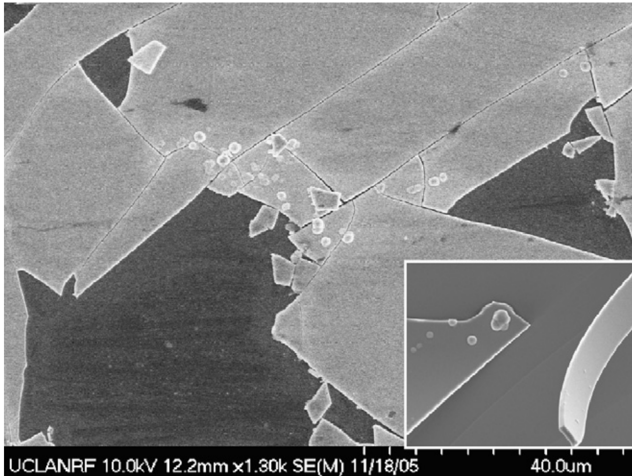

Fig. 10. Scanning electron micrographs of an undoped ZnO film grown by CVD with O_2 at 100 °C, which has cracked and lost adhesion.

diameter. The increased number of these circular grains correlates well with the increased resistivity of the film.

3.5. Film stress

It has been found that ZnO films grown by thermal CVD with O_2 tend to pop off the substrate at film thicknesses greater than 400 nm due to internal stress. This suggests that there may be an adhesion problem for these films, since PECVD grown films with CO_2 could be deposited to a thickness exceeding 2.0 μm, and no peeling of the film is observed either on glass or silicon wafers. Thick films grown by either method tend to show small cracks and fissures, however. As an example, shown in Fig. 10 is a scanning electron micrograph of a film grown by thermal CVD with O_2 at 100 °C.

4. Discussion

A comparison of the SEM images of the low- (cf. Fig. 7) and high-resistivity samples (cf. Figs. 8 and 9) reveals a stark contrast in film morphology. The more conductive sample grown at 224 °C exhibits larger grains, with fewer grain boundaries in a given cross-section. This morphology type should lead to higher carrier mobilities, since previous studies have found that grain boundary scattering is the primary mode for recombination of free carriers in polycrystalline, doped zinc oxide [14]. The increased carrier mobility would explain the lower average resistivity measured for samples grown at 224 °C by PECVD using CO_2.

For the ZnO films grown by PECVD, the changes observed in film properties with process conditions may be related to the effects of surface diffusion. It has been established that the surface diffusion length, Λ, adheres to the following relationship in the burial or high-growth-rate regime [15]:

$$\Lambda \propto \sqrt{\frac{T n_0}{J_r}} \exp(-E_s/2RT), \quad (1)$$

where n_0 is the adsorption site density (cm^{-2}), J_r is the deposition flux in (molecules/cm^2 s), and E_s is the energy barrier for diffusion (J/mol). Eq. (1) shows that the mobility of the surface species should increase rapidly with temperature following an Arrhenius relationship, whereas it should decrease with deposition flux, J_r. The deposition flux is, in turn, proportional to the diethylzinc partial pressure. By allowing adsorbed species to diffuse greater distances before being buried, there is an increased probability that they will find an appropriate adsorption site and contribute to the preferred vertically collimated grain growth. The trends reported in Figs. 4 and 6 are consistent with this interpretation, where one sees improving film properties at higher substrate temperatures and lower diethylzinc partial pressures.

5. Conclusions

The atmospheric pressure PECVD of aluminum-doped zinc oxide has been demonstrated for the first time. A resistivity of $3.3 \times 10^{-2}\,\Omega$cm and absorption coefficient of 0.04 μm^{-1} was recorded for ZnO films grown by PECVD at 20-mTorr DEZn, 1.0 Torr CO_2, 800 Torr He, a TMAl/DEZn ratio of 1:100, 75 W RF power, and 225 °C. Under these conditions, the maximum deposition rate was 72 nm/min. For ZnO deposition at low temperature, atmospheric pressure PECVD shows clear advantages over thermal CVD.

Acknowledgments

This research was made possible by funding from the Energy Innovations Small Grant (EISG) program of the California Energy Commission. The authors would also like to acknowledge Surfx Technologies, LLC, for donating the plasma source used in this project and the support of Dr. Steve Babayan in the setup and troubleshooting of this source. Finally, we would like to thank Dr. Daniel Law at Spectrolab for obtaining the raw UV–visible spectroscopic data.

References

[1] E. Fortunato, P. Nunes, A. Margues, D. Costa, H. Aguas, I. Ferreira, M.E.V. Costa, R. Martins, Adv. Mater. Forum I (2002) 571.
[2] M. Fonrodona, J. Escarré, F. Villar, D. Soler, J.M. Asensi, J. Bertomeu, J. Andreu, Sol. Energy Mater. Sol. Cells 89 (2005) 37.
[3] Th. Gruber, C. Kirchner, A. Waag, Phys. Stat. Sol. (b) 2 (2005) 841.
[4] B.S. Li, Y.C. Liu, Z.Z. Zhi, D.Z. Shen, J.Y. Zhang, Y.M. Lu, X.W. Fan, X.G. Kong, J. Vac. Sci. Technol. A 20 (5) (2002) 1779.
[5] R. Groenen, J. Löffler, J.L. Linden, R.E.I. Schropp, M.C.M. van de Sanden, Thin Solid Films 492 (2005) 298.
[6] T. David, S. Goldsmith, R.L. Boxman, Vac. Tech. Coat. 6 (4) (2005) 40.
[7] J. Hu, R.G. Gordon, J. Appl. Phys. 71 (2) (1992) 880.
[8] T.J. Coutts, J.D. Perkins, D.S. Ginley, T.O. Mason, in: The 195th Meeting of the Electrochemical Society, NREL/CP-520-26640, 1999, pp. 1–15.

[9] M. Moravej, S.E. Babayan, G.R. Nowling, X. Yang, R.F. Hicks, Plasma Sources Sci. Technol. 13 (2004) 8.
[10] G.R. Nowling, M. Yajima, S.E. Babayan, M. Moravej, X. Yang, W. Hoffman, R.F. Hicks, Plasma Sources Sci. Technol. 14 (2005) 477.
[11] G.R. Nowling, S.E. Babayan, V. Jankovic, R.F. Hicks, Plasma Sources Sci. Technol. 11 (2002) 97.
[12] M. Moravej, S.E. Babayan, X. Yang, G.R. Nowling, R.F. Hicks, J. Appl. Phys. 96 (2004) 7011.
[13] A.P. Chatterjee, P. Mitra, A.K. Mukhopadhyay, J. Mater. Sci. 34 (17) (1999) 4225.
[14] K. Ellmer, J. Phys. D 34 (2001) 3097.
[15] D.L. Smith, Thin-Film Deposition, McGraw-Hill, New York, 1995.